



Artificial Neural Networks Based Prediction of Penetration in Activated Tungsten Inert Gas Welding

ORCID: Samarendra Acharya: <https://orcid.org/0000-0002-8337-8839>

ORCID: Debasish Gonda: <https://orcid.org/0000-0002-7300-2846>

ORCID: Santanu Das: <https://orcid.org/0000-0001-9085-3450>

Samarendra Acharya¹, Debasish Gonda², Santanu Das³

^{1,2,3}Mechanical Engineering Department

Kalyani Govt. Engineering College, Kalyani- 741235, West Bengal, India

¹Department of Mechanical Engineering

Global Institute of Management and Technology, Krishnanagar, Nadia, West Bengal

Email: ¹samarendraacharya2012@gmail.com

²debashisgonda.me@gmail.com, ³sdas.me@gmail.com

DOI : 10.22486/iwj.v57i1.223729

Abstract

Using GTAW, or tungsten inert gas (TIG) welding, weld penetration is usually lesser than the other arc welding processes. ATIG (Activated-flux TIG) welding can be a good alternative to provide deep penetration, and hence, improved productivity. In this work, 304L SS plate of 8 mm thickness was used as base plate, and a flux with a mixture of SiO₂, MnO₂ and MoO₃ was used as a ternary flux in the ratio of 1:1:2. A 2-factor 3-level response surface methodology of central composite design was considered for designing experimental runs. Back Propagation (BP) type Artificial Neural Networks (ANN) model was developed to assess penetration in ATIG welding by using heat input and pulse frequency as the two process parameters. The ANN chosen has 2-10-1 network structure. Results show that the predicted values through ANN are conforming quite well to the experimentally obtained penetration, and hence, the applicability of ANN.

Keywords: Welding, Activated Tungsten Inert Gas Welding, ATIG, Artificial Neural Networks, ANN, NN, Prediction, Depth of Penetration.

1.0 INTRODUCTION

Shallow penetration in case of TIG welding could be overcome by applying a thin layer of activating flux over the surface of base plate prior to welding in case of ATIG welding as stated by Howse DS and Lucas W [1]. They also stated that arc constriction effect is the main responsible mechanism to cause deeper penetration as compared to increase of temperature dependent surface tension gradient which is known as reversed Marangoni effect.

Gurevich et al. [2], in 1965 first introduced the idea of activated flux TIG welding. After that a slow progress was seen until the beginning of 21st century when several extensive research works were done and still continuing. Different espousers [3-6] worked with different component of flux in single or a hybrid flux mixture in different proportions to increase productivity as well as deeper penetration. It was revealed that flux

proportions played a vital role to cause deeper penetration. Researchers showed that 10-12 mm of penetration had been achieved by applying activated flux TIG welding.

Mainly two mechanisms which are responsible to cause deeper penetration, one is reversed Marangoni effect and the other is arc constriction effect [7]. Some of the advantages claimed by researchers in ATIG welding focussed on:

- 1) maximization depth of penetration over 2-3 mm depth of penetration achieved by conventional TIG welding
- 2) lowering distortion due to narrow arc and reduced heat input for constant depth of penetration
- 3) restricting heat affected zone due to constriction of arc
- 4) minimisation of the problem of incompatibility of weld penetration due to cast-to-cast material variations.

Bhattacharya [8] reported that in ATIG welding, arc and metal flow behavior was controlled by arc constriction effect and

reversed Marangoni effect. They showed that due to the presence of activated fluxes such as SiO_2 , TiO_2 , CrO_3 and MoS_2 , the depth of penetration was achieved more than plate thickness. They explained that due to increase of oxygen concentration in the weld pool in presence of activated fluxes, heat density increases and consequently depth of penetration also increased.

In the next year, Roy et al. [9] experimented on AISI 316 stainless steel plate of thickness 5 mm by applying autogenous bead-on-plate welding. The authors used binary flux mixture comprising of SiO_2 and TiO_2 in the ratio of 1:1, 1:4 and 4:1 and compared to that of weldment without flux. Electrode tip distance and welding speed were kept constant at 5 mm and 120 mm/min respectively. Current used was DCSP of values 90A, 100A and 110 A. Another group, Ahmed et al. [10] used Response Surface Methodology (RSM) in TIG welding. DOP was taken as the response and Welding Current, Welding Voltage, Welding Speed and Pulse-on time were used as the input. Full factorial Central Composite Design (CCD) was used for the analysis. Five levels of each of the input were taken in the experiment. The DOP was most affected by the welding speed.

Vora et al. [11] investigated on base material SA 516 Gr.70 and compared the experimental values with the predicted values by applying two optimization technics such as Jaya algorithm and Teaching-learning-optimization technique (TLBO). As input parameters they used electrode gap, welding current and welding speed by taking three levels of each. They used TiO_2 as flux. Maximum depth of penetration was achieved as 8 mm. It was stated that the experimental values were in close proximity with that obtained by the two optimization techniques as mentioned. An attempt was made by Sivakumar et al. [12] taking the base material as Inconel 625. Response surface design method was used by taking 3 factors and 5 levels. As input parameters, they choose welding current, welding speed and arc gap. Maximum depth of penetration was achieved as 6.5 mm. Here the two optimization technics, such as Grey Relational Analysis (GRA) and TOPSIS model were used to validate the experimental results. It was stated that GRA showed better result than TOPSIS. SEM and XRD were used for analyzing the results.

Acharya et al. [13] stated the impact of various activating fluxes on different materials such as aluminium alloy, magnesium alloy, stainless steel and dissimilar metals. Reversed Marangoni effect and arc constriction effect are mainly responsible to cause deep penetration. It was recommended that three kinds of polarity of current were used in ATIG welding such as DCSP (direct current straight polarity) or DCEN (direct current electrode negative), DCRP (direct current reverse polarity) or DCEP (direct current electrode positive) and AC (alternating current). ATIG welding is highly

recommended to industries for increase of depth of penetration as well as productivity.

Chandrasekar et al. [14] reported that fusion welding to be the best suited method for industry based application. ATIG process associated with comparatively less bead width and high depth of penetration as well as less heat input. Individual materials are treated with Proper flux material to get the desired benefit from ATIG welding. Unni et al. [15] experimented on 316 LN steel during ATIG welding. They compared the experimental results with 3 D model. ANSYS FLUENT was used for creation of the model. It was found that if the oxygen simulation levels vary above 150 ppm, inward flow of molten pool occurred. The opposite phenomenon occurred when the oxygen simulation level falls below 150 ppm. It was found that the stimulated results matched with the experimental ones.

Niagaj [16] experimented on ATIG welding by considering four different types of steel by taking five different types of fluxes. The types of steels are Unalloyed Carbon Steel, Fine Grained Steel, Weld on 300 steel and AISI 304L steel. Five different fluxes were considered such as Cr_2O_3 , TiO_2 , SiO_2 , Fe_2O_3 , NaF and AlF_3 . It was also stated that method of production of steel also played a vital role in creating large depth of penetration. It was also revealed that pure metal can produce higher depth of penetration. NaF and AlF_3 were stated to have little effect on AISI 304L and more effective for fine grained steel. In another work conducted by Vora et al. [17], they reported the effect of TiO_2 flux on 6 mm thickness of SA 516 Gr. 70 carbon steel material. In this work, welding current, arc length and torch travel speed were selected as input parameters and responses were taken such as heat input, heat affected zone, D/W ratio and depth of penetration. Process parameters as well as responses were optimised by the combinations of two algorithms namely RSM (Response Surface Methodology) and HTS (Hough Transform Statistics) algorithms.

The Analytical hierarchy process (AHP) was effectively applied by Acharya et al. [18] for optimization of input parameters and responses with the experimental values conducted by Magudeeswaran et al. (2014). 9 experimental runs were conducted by taking the input parameters such as heat input, weld speed and electrode gap and consequently, depth of penetration as response. They used AdorAeTIG as flux and UNS32205 duplex stainless steel as base metal during experimentation. The AHP, a multi-criteria decision making tool was used to explore the optimal depth of penetration and productivity benefits in ATIG welding. Reversed Marangoni effect and arc constriction effect could be the main mechanism causing deep penetration in ATIG welding..

Artificial neural network (ANN) was successfully applied by Ates [19] to predict the parameters of GMAW process. In this ANN model, gas mixtures were the input parameters and

output parameters were the mechanical properties such as impact strength, tensile strength, elongation and hardness of weld metal, etc. For training purposes, extended delta-bar delta learning algorithm was used for controlling ANN model. The results based on ANN model were in good accord with that obtained by calculated ones.

Pal et al. [20] carried out an experiment on designing based on response surface methodology in pulsed metal inert gas welding. A multi-layer neural network was implemented to predict ultimate tensile stress of weld joint. Pulse voltage, back-ground voltage, pulse duration, pulse frequency, wire feed rate and welding speed, and RMS values of weld current and voltage were considered to be input variables and UTS was chosen output variable. It was reported that the output obtained through multilayer neural network model showed better result than that obtained through multiple regression model analysis.

Chandrasekhar, N. and Vasudevan, M. applied [21] an efficient model combining ANN and genetic algorithm (GA) for evaluating optimal process parameters to achieve favourable bead width and penetration in activated flux TIG (A TIG) welding of 304 LN and 316 LN stainless steel. First ANN models matching up bead geometry, viz. bead width and depth of penetration, with ATIG process parameters, viz. current, voltage, welding speed, and arc gap were introduced separately for 304 LN and 316 LN stainless steels. Then GA code was implemented in which main function was evaluated using ANN models. Close matching was observed between weld-bead geometry obtained using the GA optimized process parameters with the observed ones. Genetic algorithm based optimisation model was developed [22] for optimisation of bead geometry in 304LN and 316 LN steels.

Saha and Das as well as Saha et al. [23-26] reported remarkable improvement of penetration in ATIG welding with or without using pulsed TIG by varying different welding process parameters and employing single and double flux mixtures. Single TiO₂ flux and some other combinations of fluxes with TiO₂ as one of their compositions were found to give

beneficial effect in terms of enhancing productivity through improved penetration thereby requiring less number of welding passes.

In this work, 304L Stainless Steel plate of 8 mm thickness was used as base metal, and a flux with the mixture of SiO₂, MnO₂ and MoO₃ was used as a ternary flux in the ratio of 1:1:2. A 2-factor 3-level response surface methodology (RSM) of central composite design was considered for designing the experiment. Back Propagation (BP) type Artificial Neural Networks (ANN) model would be developed to assess penetration in ATIG welding by using heat input and pulse frequency as the input variable to find the applicability of ANN.

2.0 DETAILS OF EXPERIMENTATION

The experiment is conducted taking base metal SS304L with size 100 x 75 x 8 mm. During experimentation of ATIG welding, autogenous butt welding is carried out taking zero root gap. At first, bead-on-plate welding is conducted for trial run and then ATIG welding is done by taking a ternary flux mixture SiO₂, MnO₂ and MoO₃ in the ratio of 1:1:2.

In the present work, 13 pairs of welding specimens were used. At first, cleaning of the edges with alcoholic solution were done after proper grinding with the help of pedestal grinding wheel. For proper alignment of two work pieces with zero root gap, clamping was done. After proper fixing i.e. proper alignment one copper plate was allowed to affix under the joint area. This was done to disperse the heat generated and consequently to reduce the heat affected zone. After that, 13 experiments were done with autogenous butt welding with zero root gaps. 2% thoriated tungsten electrode with 3 mm diameter (air cooled) is used to conduct the experiment. **Table 1** and **Table 2** show the details of experimental runs performed. Weld joint of all the experimental runs were shown in **Fig. 1**. After welding, all the welded plates were cooled in ambient temperature. Welded portion were cut by an abrasive cutter and followed by belt grinding, disc grinding and polishing are done. Finally, weld bead geometry is observed under microscope. A typical bead is shown in **Fig. 2**.

Table 1 : Range of input variables for welding

Sl. No.	Variables	Unit	Minimum Value	Maximum Value
1	Heat Input	kJ/mm	1.281	2.767
2	Pulse Frequency	Hz	80	160

Table 2 : Details of experimental runs

Sl. No	Input parameters		Response
	Heat input (kJ/mm)	Pulse frequency (Hz)	Depth of penetration (mm)
1	1.281	80	3.07
2	2.767	80	4.05
3	1.281	160	3.55
4	2.767	160	4.42
5	1.281	120	3.22
6	2.767	120	4.16
7	1.470	80	3.78
8	1.470	160	4.16
9	1.470	120	3.744
10	1.470	120	3.720
11	1.470	120	3.739
12	1.470	120	3.740
13	1.470	120	3.745

Input parameters were selected as heat input and pulse frequency. The design was considered with 2 factors and 3 levels following RSM (Response surface methodology) with CCD (Central composite design). Output parameters selected as depth of penetration (**Fig.2**). 99.9% pure argon gas (99.9%) was applied as the shielding gas and 75° gun angle was set for the whole experiment. 5 mm distance from electrode to work piece was kept as constant. Gas pressure used was 2.5 bar. A heat input (HI) of 2.767 kJ/mm, pulse frequency of 160 Hz was found to be the optimal condition of ATIG welding.

3.0 THE ANN APPLIED

13 data sets were obtained from the experimental work and these data sets are used to build up the Artificial Neural Networks (ANN) of 2-10-1 structure. Variations of hidden nodes in a single hidden layer were carried out and consequently to find minimum training error, finally the structure is found with 10 hidden nodes in a single hidden layer. The data set consists of input process parameters, i.e. heat input and pulse frequency and the corresponding output parameter, or response, that is, depth of penetration (P). The work is to forecast these bead geometry parameter with the help of ANN. Levenberg-Marquardt training algorithm is used. As Performance Function, mean square error is used. Here, in the ANN model, 70% data sets, i.e. 9 sets of data, are used for training purpose, 15% data, i.e. 2 sets of data, are kept for validation and 15% of data, i.e. 2 sets of data, are employed for testing.

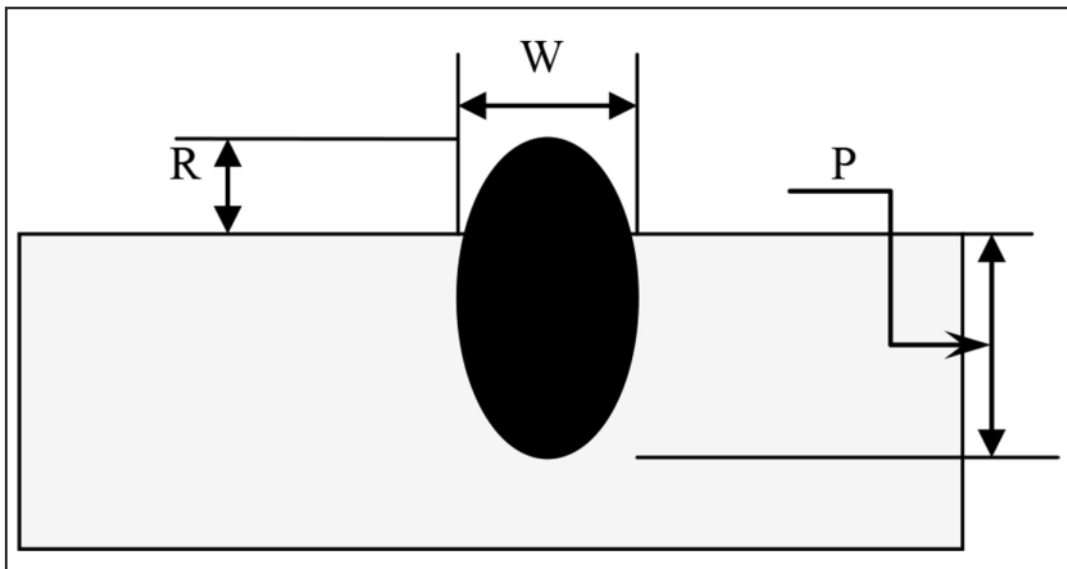


Fig. 2: A typical bead geometry
[R= Reinforcement, W= BW, P= Depth of penetration]














		
a. Weld joint exp. No. 1	b.Weld joint exp. No.2	c.Weld joint exp. No. 3
		
d. Weld Joint exp. No.4	e. Weld Joint exp. No.5	f. Weld Joint exp. No.6
		
g. Weld Joint exp. No.7	h. Weld Joint exp. No. 8	i. Weld Joint exp. No. 9
		
j. Weld Joint exp. No.10	k. Weld Joint exp. No. 11	l. Weld Joint exp. No. 12
		
m. Weld Joint exp. No.13		

Figure 1 : ATIG welded specimen

Table 3 : Summary of processes (Training, Validation and Testing)

Process	Observation	MSE	R
Training	9	0.0864	0.8781
Validation	2	0.2707	-1.0000
Test	2	0.1560	1.0000

In this model, the values of MSE (mean square error) in training, validation and testing are nearly close to zero and the values of R (coefficient of correlation) in training, validation and testing are 1 and nearly close to 1. So, this ANN model is

taken into consideration for prediction purpose. A value of R makes sense very close to 1 as mentioned in **Table 3** for different processes such as training, validation and testing, because it measures goodness-of-fit. The statistical implication states that any changes in the independent variables reimburse with the dependent variables.

4.0 REGRESSION PLOT ANALYSIS OF EXPERIMENTAL NETWORK

Close correlation between training, validation and testing stages as shown by Regression plot analysis of experimental network and depicted in **Fig. 3**. It can be seen that the regression value is close to 1; so the model constructed is significant.

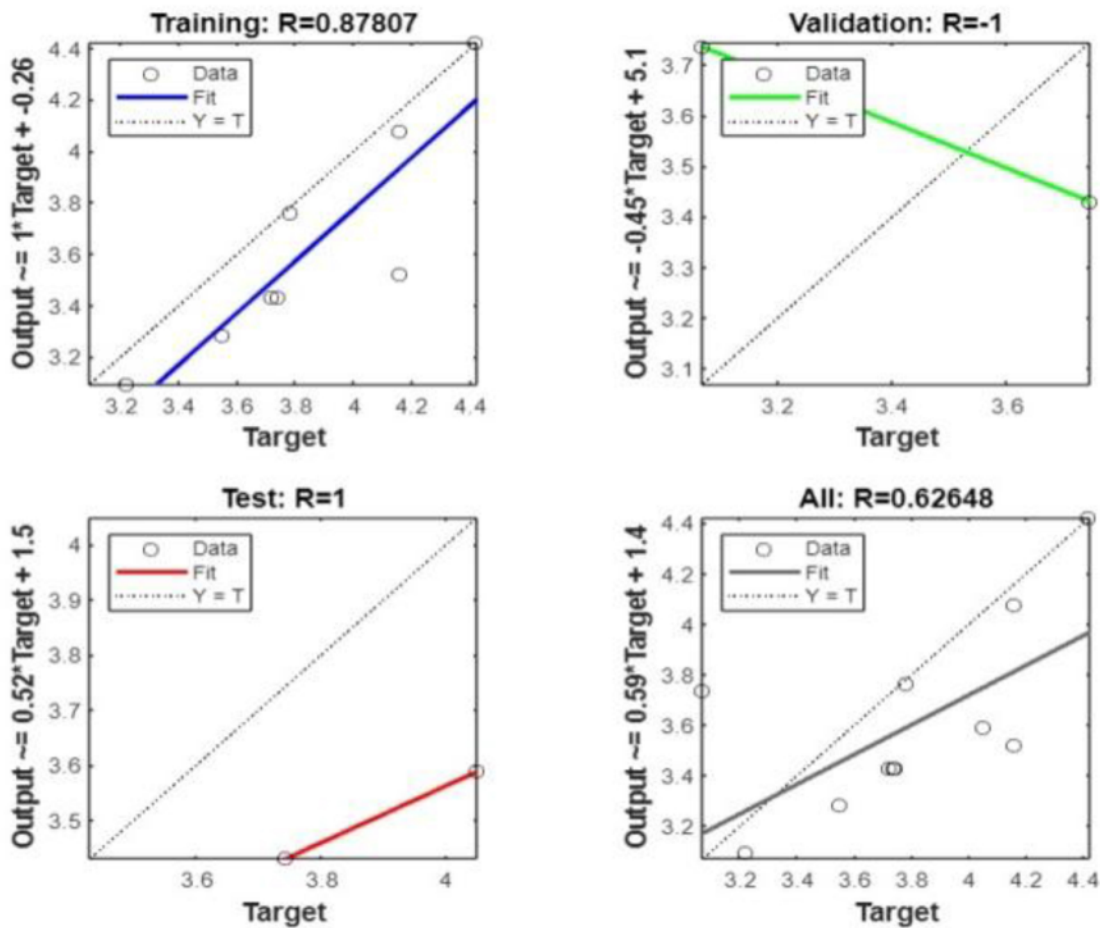


Figure 3 : Regression plot analysis

5.0 RESULTS AND DISCUSSION

Table 4 and **Fig. 4** show the correlation of experimental and predicted depth of penetration values of the 13 experimental runs, Commensuration between the predicted values and the experimentally observed values of bead geometry (P) can be seen with some fluctuations at some experimental runs. By varying no. of training data sets and no. of hidden layers and hidden nodes by trial and error method, authors forecast the output keeping fixed the input and output nodes. Some fluctuations are observed between experimental and predicted values using ANN and it is not uncommon.

Authors elucidate from **Fig. 4** that fluctuations between experimental and predicted data are fairly small, and hence, ANN. can be applied successfully.

If more data sets are considered, prediction with ANN model may be better with lesser estimation error. Again somehow no. of hidden layers may be more than 1, and then there is a question of checking value of training error if it sets off lesser than the single hidden layer ANN model.

Graphical representation of the attainment in the stage for validation with the data assigned for validation is shown in Fig. 5. At the epoch 1, the best validation exhibition is observed giving the minimum forecasting error.

Table 4 : Depth of penetration (predicted and experimental) in mm

Sl. No.	P (Experimental)	P (Predicted)
1	3.07	3.735
2	4.05	3.5881
3	3.55	3.2816
4	4.42	4.424
5	3.22	3.0952
6	4.16	4.0776
7	3.78	3.761
8	4.16	3.5216
9	3.744	3.43
10	3.720	3.43
11	3.739	3.43
12	3.740	3.43
13	3.745	3.43

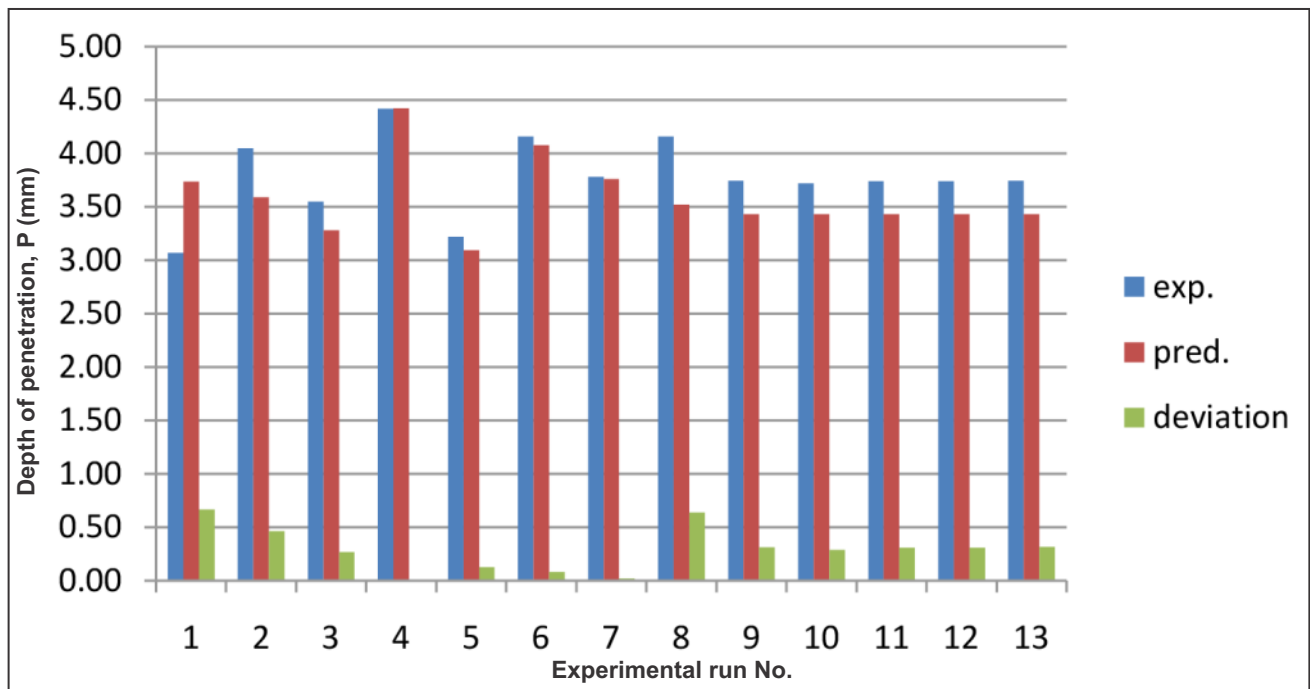


Fig. 4 : Bar chart of experimental and predicted depth of penetration with deviation

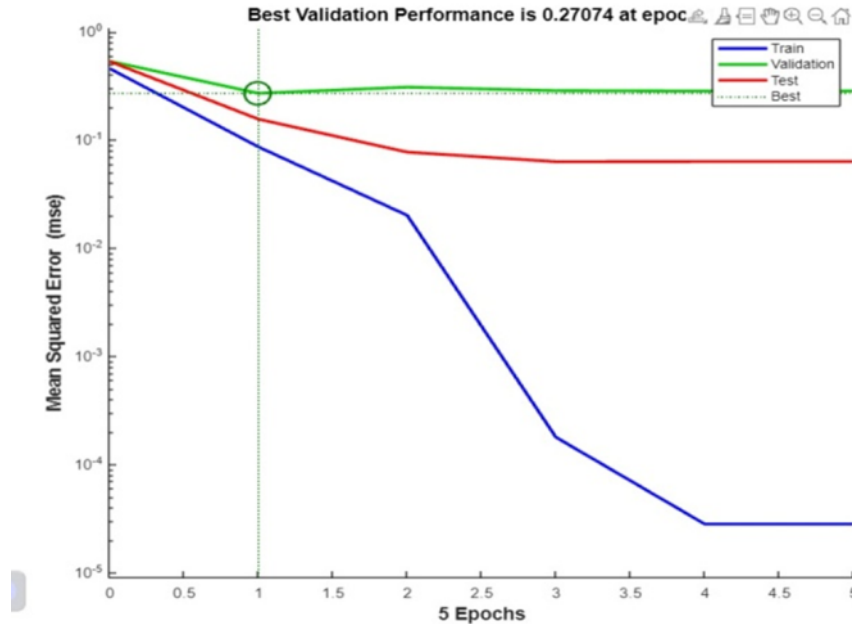


Fig. 5 : Graph of best validation performance

6.0 CONCLUSION

In this work, a new ternary flux mixture (SiO_2 , MnO_2 and MoO_3) mixed with 1:1:2 fixed proportions was attempted to get large depth of penetration. A penetration of 4.42 mm was achieved with a heat input of 2.767 kJ/mm, and pulse frequency of 160 Hz.

Forecasted depth of penetration in ATIG welding achieved by the use of artificial neural networks is found to be very close to that of the experimental value. Although some deviations are observed at certain cases. So, it can be accorded that the ANN can be suitably and successfully implemented as an estimation tool.

REFERENCES

- [1] Howse DS and Lucas W (2000); Investigation into arc constriction by active fluxes for tungsten inert gas welding, *Sc and Tech of Welding and Joining*, 5, pp.189-193.
- [2] Gurevich SM, Zamkov VN and Kushnirenko NA (1965); Improving the penetration of titanium alloys when they are welded by argon tungsten arc process, *Avtomatic Svarka*, 9, pp. 1-4.
- [3] Lin HL and Wu TM. (2012); Effects of Activating Flux on Weld Bead Geometry of Inconel 718 Alloy TIG Welds, *Materials and Manufacturing Processes*, 27, pp.1457-1461.
- [4] Modenesi PJ, Âquio R, Ario, A. and Pereira IM (2000); TIG welding with single-component fluxes, *Journal of Materials Processing Technology*, 99, pp. 260-265.
- [5] Huang HY (2010); Effects of activating flux on the welded joint characteristics in gas metal arc welding, *Materials and Design*, 31, pp. 2488-2495.
- [6] Tseng KH and Hsu CY (2011); Performance of activated TIG process in austenitic stainless steel welds, *Journal of Materials Processing Technology*, 211, pp. 503-512.
- [7] Cai Y, Luo Z, Huang Z, and Zeng Y (2016); Effect of cerium oxide flux on active flux TIG welding of 800 Mpa super steel, *Journal of Materials Processing Technology*, 230, pp. 80-87.
- [8] Bhattacharya A (2016); Revisiting Arc, Metal Flow Behavior in Flux Activated Tungsten Inert Gas Welding, 31, pp. 343-351.
- [9] Roy S, Samaddar S, Uddin NM and Das S (2017); Effect of Activating Flux on Penetration in ATIG Welding of 316 Stainless Steel", *Indian Welding Journal*, Vol.50, pp.72-80.
- [10] Ahmad A and Alam S (2019); Parametric Optimization of TIG Welding using Response Surface Methodology, *Materials today: Proceedings*, 18, pp.3071-3079.
- [11] Vora JJ, Abhishek K and Srinivasan S (2015); Attaining Optimized ATIG Welding Parameters for Carbon Steels by Advanced Parameter-less Optimization Techniques:

- with Experimental Validation, Journal of the Brazilian Society of Mechanical Sciences and Engineering, 41, pp. 260-280.
- [12] Sivakumar J, Vasudevan M and Korra N N (2020); Systematic Welding Process Parameter Optimization in ATIG Welding of Inconel 625, Transactions of the Indian Institute of Metals, 73, pp. 555-569.
- [13] Acharya S. and Das S (2020); Effect of Activating Flux in Gas Tungsten Arc Welding, Weld Fab TechTimes, 4, pp.12-21.
- [14] Chandrasekar G, Kannan R, Prabakaran MP and Ganesamoorthy R (2020); Effect of Activating Flux (Metal Oxide) on the Weld Bead Nomenclature of Tungsten Inert Gas Welding Process - A Review, IOP Conf. Series: Materials Science and Engineering, 988, 012084.
- [15] Unni KA and Vasudevan M (2020) ; Numerical Modelling Fluid Flow and Weld Penetration in Activated TIG Welding, Materials Today: Proceedings, 27, pp. 2768-2773.
- [16] Niagaj J (2021), Influence of Activated Fluxes on the Bead Shape of ATIG Welds on Carbon and Low Alloy Steels in Comparison with Stainless Steel AISI 304L, Metals, 11, pp. 530-543.
- [17] Vora J, Patel VK, Srinivasan S, Chaudhari R, Pimenov DY, Giasin K and Sharma S (2021); Optimization of Activated Tungsten Inert Gas Welding Process Parameters Using Heat Transfer Search Algorithm: With Experimental Validation Using Case Studies, Metals, 11, pp.1-16, 2021.
- [18] Acharya S, Gonda D and Das S (2022); Achieving Favourable Depth of Penetration and Productivity of ATIG Welds Utilising the AHP, Indian Science Cruiser, 36, pp. 17-23.
- [19] Ates H (2007); Prediction of gas metal arc welding parameters based on artificial neural networks, Materials & Design, 28, pp. 2015-2023.
- [20] Pal S, Pal SK and Samantaray AK (2008); Artificial neural network modelling of weld joint strength prediction of a pulsed metal inert gas welding process using arc signals, Journal of Materials Processing Technology, 202, pp. 464-474.
- [21] Chandrasekhar N & Vasudevan, M (2010); Intelligent Modeling for Optimization of A-TIG Welding Process, Materials and Manufacturing Processes, 25, pp.1341-1350.
- [22] Vasudevan M, Bhaduril AK, Baldev Raj and Rao KP (2007); Genetic-Algorithm based computational models for optimizing the process parameters of A-TIG welding to achieve target bead geometry in type 304 L (N) and 316 L(N) stainless steels, Materials and Manufacturing processes, 22, pp. 641-649.
- [22] Vasudevan M, Bhaduri AK, Baldev Raj and Rao KP (2007); Genetic-algorithm-based computational models for optimizing the process parameters of A-TIG welding to achieve target bead geometry in type 304L(N) and 316 L(N) stainless steels, Materials and Manufacturing Processes, 22, pp.641-649.
- [23] Saha S and Das S (2018); Investigation on the effect of activating flux on tungsten inert gas welding of austenitic stainless steel using AC polarity, Indian Welding Journal, 51(2), pp. 84-92.
- [24] Saha S and Das S (2019); Application of activated tungsten inert gas (A-TIG) welding towards improved weld bead morphology in stainless steel specimens, Annual Technical Volume of Production Division Board, The Institution of Engineers (India), IV, pp. 13-23.
- [25] Saha S and Das S (2020); Effect of polarity and oxide fluxes on weld-bead geometry in activated tungsten inert gas (A-TIG) welding, Journal of Welding and Joining, 38(4), pp. 380-388.
- [26] Saha S, Paul BC and Das S (2021); Productivity improvement in butt joining of thick stainless steel plates through the usage of activated TIG welding, SN Applied Sciences, 3(416), pp. 416/1-10.